ELSEVIER

Journal of Alloys and Compounds 446–447 (2007) 363–367

Journal of ALLOYS AND COMPOUNDS

www.elsevier.com/locate/jallcom

Phase evolution of Li_2ND, LiD and $LiND_2$ in hydriding/dehydriding of Li_3N

Wen-Ming Chien [a], Joshua Lamb [a], Dhanesh Chandra [a,*], Ashfia Huq [b], James Richardson Jr. [c], Evan Maxey [c]

[a] *Metallurgical Materials Engineering, MS 388, University of Nevada, Reno, NV 89557, United States*
[b] *Spallation Neutron Source, Oak Ridge National Laboratory, Oak Ridge, TN 37831, United States*
[c] *Intense Pulsed Neutron Source, Argonne National Laboratory, Argonne, IL 60439, United States*

Received 17 February 2007; received in revised form 22 February 2007; accepted 22 February 2007
Available online 4 March 2007

Abstract

Neutron and synchrotron studies have been performed on in situ hydriding of Li_3N. Commercial Li_3N is composed of α phase (~70 wt.%) and β phase (~30 wt.%). We have performed experiments to convert β → α, and studied in situ deuteration using neutron diffraction experiments. We found concurrent phase evolution of Li_2ND, LiD, and $LiND_2$. Mass percentages of the phases evolved as a function of time and temperature have been quantified using General Structure Analysis System (GSAS) refinement of the neutron diffraction data. The problem of formation of the stable LiD is discussed in light of decreasing of the amount of LiD phase when the temperature is increased from 200 to 320 °C during dehydriding, and in addition the concentration of Li_2ND phase increased at this temperature. Lattice parameters, volume changes, phase evolutions in wt.% as a function of temperature and time are presented.

Keywords: Li_2NH; Li_3N; $LiNH_2$; Neutron diffraction; Phase analysis

1. Introduction

Several studies have indicated complex alkali metal based hydrides, such as, lithium amide ($LiNH_2$) and lithium imide (Li_2NH) are particularly attractive as potential candidates for hydrogen storage due to their relatively high theoretical gravimetric hydrogen density (e.g., $LiNH_2$ alone has 6.5 wt.% hydrogen). Chen et al. [1] pioneered the progressive hydrogenation of lithium nitride, Li_3N, which leads to the absorption of the theoretical 11.5 wt.% hydrogen by the reaction in Eq. (1):

$$Li_3N + 2H_2 \Leftrightarrow Li_2NH + LiH + H_2 \Leftrightarrow LiNH_2 + 2LiH \quad \text{(total capacity : 11.5 wt.\% } H_2\text{)} \tag{1}$$

If only imides are considered, then the following Eq. (2) is valid.

$$Li_2NH + H_2 \Leftrightarrow LiNH_2 + LiH \quad \text{(reversible at } \sim 1 \text{ bar at } 285\,^\circ\text{C},\ 6.5 \text{ wt.\% } H_2,\ \Delta H = 45 \text{ kJ/mol)} \tag{2}$$

To increase the equilibrium pressure, Luo [2] showed that Mg additions increase the plateau pressures, Eq. (3).

$$2LiNH_2 + MgH_2 \Leftrightarrow Li_2Mg(NH)_2 \quad (32 \text{ bar at } 200\,^\circ\text{C}) \tag{3}$$

Chen et al. [1] also suggested that full reversal to Li_3N may be possible at higher temperatures (>400 °C) as per Eq. (4), which is also confounded with competing side-reactions leading to ammonia formation as in Eqs. (5) and (6) [3].

$$Li_2NH + LiH \Leftrightarrow Li_3N + H_2 \quad \text{(not easily reversible, } \sim 0.01 \text{ bar at } 255\,^\circ\text{C},\ 5 \text{ wt.\% } H_2,\ \Delta H = 165 \text{ kJ/mol)} \tag{4}$$

$$2LiNH_2 \Leftrightarrow Li_2NH + NH_3 \quad (3.7 \text{ wt.\% } NH_3,\ \Delta H = +84 \text{ kJ/mol } NH_3) \tag{5}$$

$$NH_3 + LiH \rightarrow 2LiNH_2 + H_2 \quad (5.8 \text{ wt.\% } H_2,\ \Delta H = -39 \text{ kJ/mol } NH_3) \tag{6}$$

* Corresponding author. Tel.: +1 775 784 4960; fax: +1 775 784 4316.
E-mail address: dchandra@unr.edu (D. Chandra).

0925-8388/$ – see front matter © 2007 Elsevier B.V. All rights reserved.
doi:10.1016/j.jallcom.2007.02.149

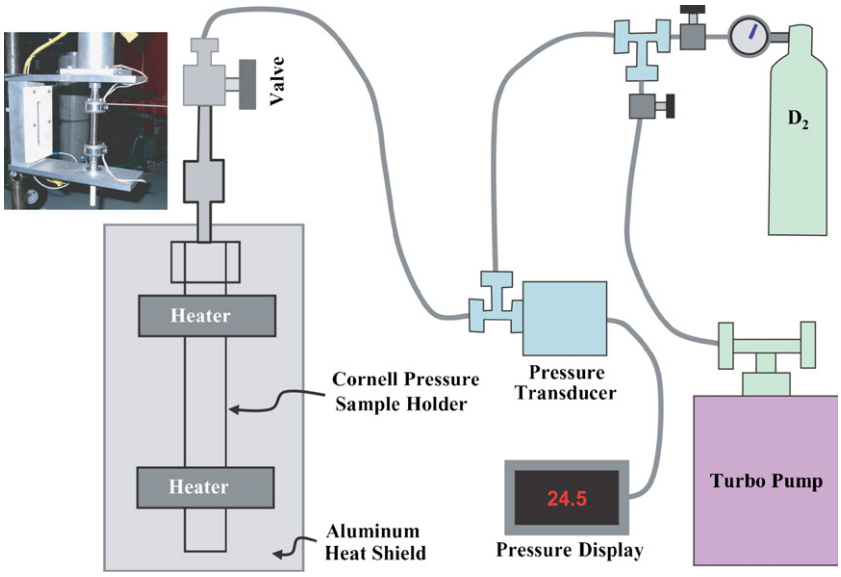

Fig. 1. Schematic of the in situ deuteriding/de-deuteriding experimental setup.

However, these hydrogenation/dehydrogenation reactions have not been shown to be reversible or to have adequate hydrogen release kinetics at moderate temperatures.

Issues with ammonia evolution were reported by Ichikawa et al. [4] who indicated that the NH_3 release is controllable; the NH_3 evolved during a first-order reaction, then is consumed in a secondary reaction shown in Eq. (6); the kinetics are very fast for this reaction. The lithium-based complex hydrides have great potential as materials for fuel cell, on-board vehicular, and other applications [5–7].

Commercial Li_3N powder is a two-phase mixture of α-Li_3N and β-Li_3N. The structure of the α phase is hexagonal with *P*6/*mmm* space group with lattice constants $a = 3.648(1)$ Å and $c = 3.875(1)$ Å ($Z = 1$) [8,9]. The β phase is a high-pressure phase, and is a hexagonal structure with $a = 3.552(1)$ Å and $c = 6.311(3)$ Å ($P6_3/mmc$, $Z = 2$) [10]. The low-temperature structural behavior studies of the α-Li_3N and β-Li_3N phases have been performed by Huq et al. [11] and Chien et al. [12] using neutron powder diffraction (NPD). The structure of Li_2NH was reported as cubic (*Fm*-3*m*) with $a = 5.0742(2)$ Å by Noritake et al. [13] using synchrotron X-ray diffraction (XRD), and by Ohoyama et al. [14] using NPD. Recently, Balogh et al. [15] reported the crystal structure and phase transformation of deuterated lithium imide (Li_2ND) using both NPD and XRD. The crystal structure of $LiNH_2$ was determined by Juza and Opp [16], and re-determined by Jacobs and Juza (single-crystal XRD) [17], Miwa et al. [18], and Yang et al. by NPD [19] as tetragonal structure with $a = 5.03442$ and $c = 10.25558$ Å (space group *I*-4).

Li-based hydrides show a high capacity for reversible hydrogen storage. However, understanding phase formation behaviors during temperature change is also important for the hydrogen storage application. In this study, we report results of NPD studies, such as phase evolution of the amide, imide, LiD, during hydrogenation of Li_3N. Also the effect of temperature on deuteriding and de-deuteriding of Li_3N.

2. Experimental

A lithium nitride sample (Li_3N, 80 mesh) was obtained from Sigma–Aldrich in the form of a powder. Time-of-flight (TOF) NPD data was collected for the Li_3N sample using the General Purpose Powder Diffractometer (GPPD) at the Intense Pulsed Neutron Source (IPNS), Argonne National Laboratory. Diffraction data were collected on all detector banks. The sample was loaded in the Inconel alloy pressure sample holder in a helium-filled re-circulating glove-box. The in situ deuteriding/de-deuteriding experimental setup is shown in Fig. 1. Deuterium gas was supplied at 2 bar during the deuteriding experiment. Rietveld refinements were performed using the General Structure Analysis System (GSAS) computer software [20,21]. To de-deuteride, for the results shown in Fig. 3, we used active evacuation via a Varian V-70 turbo pump system, backed up with a dry mechanical pump. The NPD data were acquired on two banks of detectors at IPNS (Argonne National Laboratories), every 15 min. The phases were identified first by standard search methods, and then the compositional changes were tracked using the GSAS program.

3. Results and discussions

In this study, we performed both diffraction studies on the pre-treated α phase Li_3N sample as well as α + β Li_3N commercial powders. At room temperature, the NPD data show that the commercial Li_3N sample contains two different phases: 65 wt.% α-Li_3N phase and 35 wt.% β-Li_3N phase. Isothermal in situ deuteriding NPD data was taken at 200 °C at 2 bar D_2 pressure. Isothermal evolution (wt.%) of different phases as a function of time is shown in Fig. 2. Initially, as the temperature was equilibrated to 200 °C, the only change observed in the diffraction pattern was β-Li_3N transforming to α-Li_3N phase (region 1); the α-Li_3N phase increases from 65 to 79 wt.% with a corresponding decrease in the mass of the β phase. In region 2, the hydride phases Li_2ND and LiD begin to appear. Concurrently, there is a decrease in the mass of the α-Li_3N phase, suggesting that the α-Li_3N is converting to Li_2ND and LiD. The β-Li_3N phase concentration continues to decrease in region 2. The evolution of the amide $LiND_2$ phase was observed after ~145 min, in region 3. It can be noted that in region 3, concentrations of $LiND_2$ and LiD are greater than that of Li_2ND,

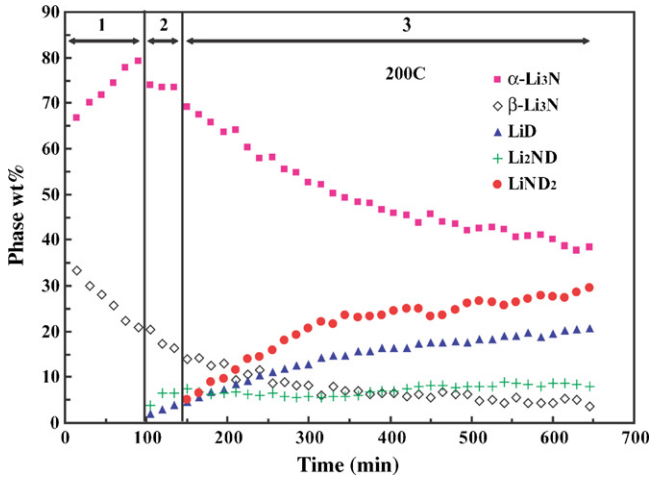

Fig. 2. Isothermal in situ deuteriding NPD results (at 200 °C and 2 bar D_2 pressure of the commercial Li_3N sample (α-Li_3N and β-Li_3N) show the different amounts of phase formation as a function of time.

indicating either direct formation of $LiND_2$ from Li_3N or rapid transformation of $Li_2ND \rightarrow LiND_2$ during these multiple concurrent transformations. It does appear that, as the amount of α-Li_3N phase decreases, there is a corresponding increase in the amount of $LiND_2$ formed. The reactions in regions 1–3 at 200 °C are summarized in Table 1.

Another in situ deuteriding/de-deuteriding experiment was performed by using the pre-treated Li_3N sample which contained only the α-Li_3N phase; the β-Li_3N to α-Li_3N transformation occurs readily above 250 °C. The results are presented for the deuteration and de-deuteration in Fig. 3. Deuteriding was performed at room temperature, 150, 200, and 250 °C. As expected, the α-Li_3N phase is stable up to 150 °C. As temperature was increased from 150 to 200 °C, (from ∼19 to 30 h) the hydride phases, Li_2ND, LiD, and $LiND_2$ form simultaneously under these conditions (2 bar of deuterium pressure). Also note that as the temperature is raised there is time lag to equilibrate. The amount of Li_2ND phase increases to ∼19 wt.%, the LiD phase to ∼21 wt.%, and the $LiND_2$ phase ∼14 wt.% after isothermally holding temperature at 200 °C for 9 h. From Fig. 3, it can seen that the α-Li_3N phase concentration decreases rapidly in the 200 and 250 °C regions at the deuteriding region, and only ∼10 wt.% is residual after 12 h of isothermal holding at 200 °C. In the 250 °C deuteriding region, initially, the amount of the Li_2ND phase formed increases rapidly, and then decreases due to the formation of the $LiND_2$ and LiD phases. It can also be noted that the formation of LiD phase continues to increase during deuteration between 200 and 250 °C, while the Li_2ND decreases and $LiND_2$ increases with a possible saturation at 40 h; with 25 wt.% of Li_2ND, 37 wt.% LiD, and 28 wt.% $LiND_2$. In the 200 °C region, there is a tendency to form Li_2ND and LiD phases in preference to $LiND_2$, similar to what we observed in Fig. 2. The total amount of hydrogen storage is calculated to be 7.26 wt.% at the end of 44 h.

Table 1
Summary of isothermal transformations in each region at 200 °C

Region 1	Region 2	Region 3
Up to ∼100 min	100–145 min	145–650 min
β-$Li_3N \rightarrow$ α-Li_3N	β-$Li_3N \rightarrow$ α-Li_3N	β-$Li_3N \rightarrow$ α-Li_3N
	α-$Li_3N \rightarrow Li_2ND + LiD$	α-$Li_3N \rightarrow Li_2ND + LiD$
		$Li_2ND \rightarrow LiND_2$ (rapid)

The neutron data indicate a total storage of 7.26 wt.% of hydrogen after 44 h at 255 °C. Our recent work at 255 °C showed that at 2 bar, the material has an effective equilibrium capacity of 8.7 wt.%. Four grams of material was used in the NPD studies, indicating that 0.29 g of hydrogen was stored, or 83% of the material's potential capacity. The deuteration wt.% capacity of the materials was converted to hydrogen capacity.

The overall hydrogen absorption reaction of Li_3N can be obtained from Eq. (1) as:

$$Li_3N + 2H_2 \leftrightarrow LiNH_2 + 2LiH$$

The Gibbs free energy of the ongoing reaction in our case at a hydrogen pressure of 2 bar, can be obtained using the following

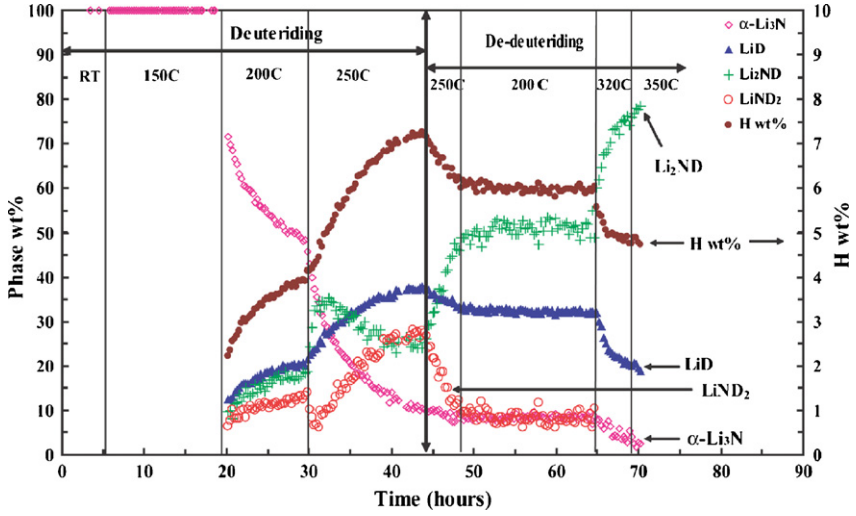

Fig. 3. The phase evolutions of the in situ deuteriding and de-deuteriding of the pure α-Li_3N sample as a function of temperature and time.

equation:

$$\Delta G = \Delta G^{\circ} + RT \ln K_{P=2\,\text{bar}}$$
$$= -RT \ln K_{P\,\text{at}\,x=7.26\,\text{wt.\%}} + RT \ln K_{P=2\,\text{bar}} \quad (7)$$

As Li_3N, $LiNH_2$, and LiH are all solid species, their activities are assumed to be equal to 1. The equilibrium constant for this reaction is estimated to be:

$$K_P = \frac{a_{LiNH_2} a_{LiH}^2}{a_{Li_3N} p_{H_2}^2} = \frac{1}{p_{H_2}^2},$$

and if the imposed pressure is 2 bar then

$$\Delta G = -RT \ln \left(\frac{1}{p_{H_2}^2} \right)_{p_{eq}} + RT \ln \left(\frac{1}{p_{H_2}^2} \right)_{p=2\,\text{bar}} \quad (8)$$

Our neutron data showed ~7.26 wt.% hydrogen (Fig. 3) at 250 °C, whereas our equilibrium absorption isotherms, using Li_3N as starting material taken at 255 °C, showed that at 2 bar hydrogen pressure there should be ~8.7 wt.% hydrogen stored (Fig. 4). Thus the absorption NPD and isotherm show a discrepancy of 1.44 wt.% hydrogen; although there is a small difference in temperature at which these two data sets were taken. From our isotherm (Fig. 4) we can obtain the absorption equilibrium pressure (P_{eq}) of ~0.8 bar at 7.26 wt.% hydrogen. This yields $\Delta G_{\text{Eq. (8)}} = -8.0$ kJ/mol for reaction (1), indicating that the reaction would continue to absorb the additional 1.4 wt.% hydrogen if given more time. However, we started to evacuate the system prematurely before that remaining 1.4 wt.% hydrogen was absorbed in the sample.

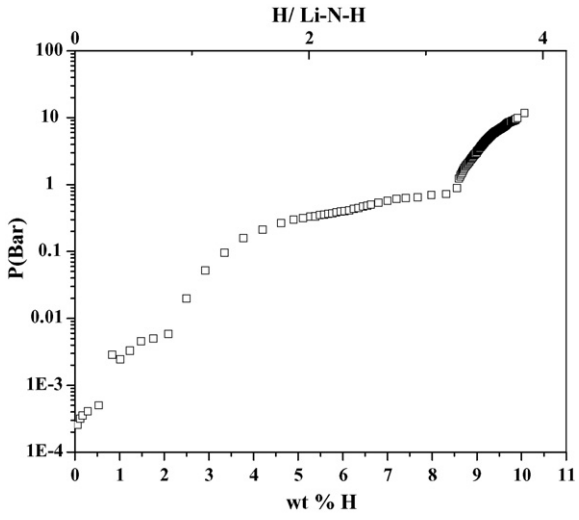

Fig. 4. Pressure-composition hydrogen absorption isotherm of Li_3N at 255 °C.

De-deuteriding was started after 44 h at 250 °C. In this 250 °C region, the amount of the Li_2ND phase increases rapidly to

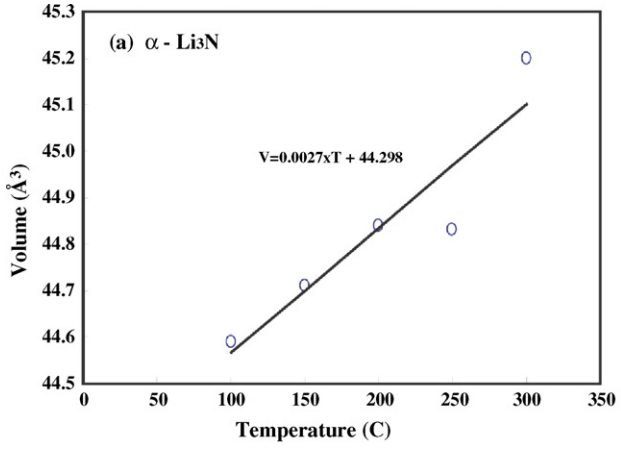

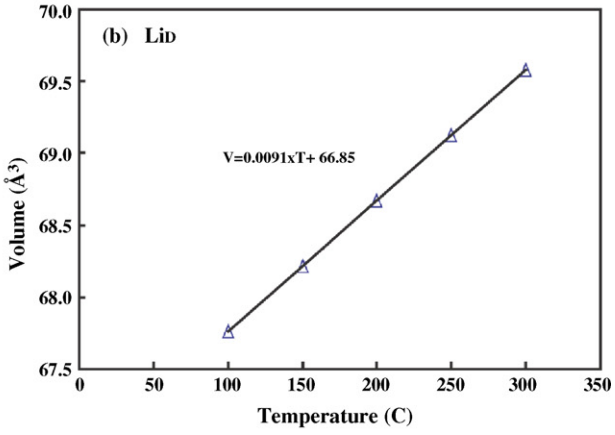

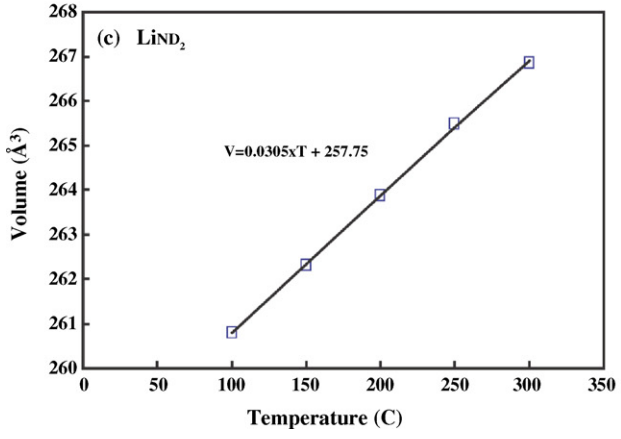

Temp	Volume (Å^3)		
	α - Li_3N	LiD	$LiND_2$
	Z=1	Z=4	Z=8
100°C	44.59	67.76	260.79
150°C	44.71	68.21	262.31
200°C	44.84	68.67	263.87
250°C	44.83	69.13	265.47
300°C	45.20	69.58	266.85

Fig. 5. The unit-cell volumes of (a) α-Li_3N, (b) LiD and (c) $LiND_2$ phases vs. temperature.

50 wt.% with a corresponding decrease of $LiND_2$ phase to 10 wt.% in 5 h. There is a much less pronounced decrease in the amount of LiD phase at this temperature; only 5 wt.% decrease observed. After 48 h, the temperature was decreased to 200 °C during de-deuteration. At this temperature the amount of Li_2ND (54%), LiD (31%), $LiND_2$ (10%) remained constant up to 65 h. Chen et al. [1] reported a rather rapid increase in hydride phase formation at 200 °C during de-hydriding, but we did not observe this behavior. We acknowledge that if we had raised the temperature by ∼10 K; we probably would have observed the changes that Chen et al. [1] had reported. It can be noted that the amount of hydrogen desorbed increased rapidly for about 2 h or so at 320 °C which is perhaps what Chen et al. observed. Increasing the temperature to 320 °C rapidly increased the amount of Li_2ND (from 54% to 76%) and decreased the amount of LiD (from 31% to 20%). No $LiND_2$ phase was measurable after 68 h; perhaps the intensity of its Bragg peaks were too low for detection above the background level. The amount of the LiD phase decreased when the de-deuteriding temperature was increased to 320 and 350 °C, and the amount of the Li_2ND phase increased as the temperature was increased during de-deuteriding. There is no $LiND_2$ phase observed upon de-deuteriding above 320 °C.

The changes in unit-cell volumes were measured at different temperatures during deuteration in equilibrated samples at different temperatures. In this experiment, the deuterated sample was heated to 250 °C, the sample holder was then sealed, and the supply of deuterium to the sample was shut off. The sample was then cooled down from 250 to 100 °C, and then reheated from 100 to 300 °C to measure the unit-cell volumes. The volume expansions as a function of temperatures of the α-Li_3N, LiD, and $LiND_2$ phases are shown in Fig. 5, and tabulated in the insert table. All these phases show an increase in unit-cell volumes, as expected. The Bragg peaks of the Li_2ND phase were not observed at these temperatures. The volume of the Li_3N phase increased from 44.59 to 45.2 $Å^3$, the LiD phase from 67.76 to 69.58 $Å^3$, and the $LiND_2$ phase from 260.79 to 266.85 $Å^3$, from 100 to 300 °C, respectively.

4. Summary and conclusions

Neutron scattering studies of deuteration of α-Li_3N showed that the different amounts of LiD, and $LiND_2$, and Li_2ND phases form during isothermal heating at different temperatures. The total amount of hydrogen storage is calculated to be 7.26 wt.% during deuteriding at 250 °C. The stable LiD phase was found to decrease slightly when the temperature is increased from 250 to 320 °C during de-deuteriding.

Acknowledgements

We thank the U.S. Department of Energy for program support through the US DOE Metal Hydride Center of Excellence (MHCoE) at Sandia National Laboratories, Livermore, CA. Argonne National Laboratory's work was supported by the U.S. Department of Energy, Office of Science, Basic Energy Sciences, under contract DE-AC02-06CH11357.

References

[1] P. Chen, Z. Xiong, J. Luo, J. Lin, K. Tan, Nature 21 (2002) 302–304.
[2] W. Luo, J. Alloys Compd. 381 (2004) 284–287.
[3] F.E. Pinkerton, J. Alloys Compd. 400 (2005) 76–82.
[4] T. Ichikawa, N. Hanada, S. Isobe, H.Y. Leng, H. Fujii, J. Phys. Chem. B 108 (2004) 7887–7892.
[5] L. Schlapbach, A. Züttel, Nature 414 (2001) 353.
[6] D. Chandra, J. Petrovic, R.G. Bautista, A. Imam, Overview of the Advanced Materials for Energy Conversion – III, Symposium in Honor of Drs. Gary Sandrock, Louis Schlapbach, and Seijirau Suda For Lifetime Achievements in Metal Hydride Research and Development; D. Chandra, J. Petrovic, R. Bautista, A. Imam, Advanced Materials for Energy Conversion III, Proceeding of the TMS Annual Symposium in San Antonio, TX, TMS Press, vol. III, 383 pages, March 2006, pp. 3–7, ISBN: 978-0-87339-610-3.
[7] D. Chandra, J.J. Reilly, R. Chellappa, J. Met. 58 (2006) 26–32.
[8] A. Rabenau, H. Schulz, J. Less-Common Met. 50 (1976) 155–159.
[9] D.H. Gregory, P.M. O'Meara, A.G. Gordon, J.P. Hodges, S. Short, J.D. Jorgensen, Chem. Mater. 14 (2002) 2063–2070.
[10] H.J. Beister, S. Haag, R. Kniep, K. Strossner, K. Syassen, Angew. Chem. Int. Ed. Engl. 27 (8) (1988) 1101–1103.
[11] A. Huq, J.W. Richardson, E.R. Maxey, D. Chandra, W. Chien, J. Alloys Compd. 436 (2007) 256–260.
[12] W. Chien, D. Chandra, A. Huq, J.W. Richardson, E.R. Maxey, S. Fakra, M. Kunz, MS&T 2006: Fund. Charact. 1 (2006) 501–507.
[13] T. Noritake, H. Nozaki, M. Aoki, S. Towata, G. Kitahara, Y. Nakamori, S. Orimo, J. Alloys Compd. 393 (2005) 264–268.
[14] K. Ohoyama, Y. Nakamori, S. Orimo, K. Yamada, J. Phys. Soc. Jpn. 74 (1) (2005) 483–487.
[15] M.P. Balogh, C.Y. Jones, J.F. Herbst, L.G. Hector Jr., M. Kundrat, J. Alloys Compd. 420 (2006) 326–336.
[16] R. Juza, K. Opp, Z. Anorg. Allgem. Chem. 266 (1951) 313–324.
[17] H. Jacobs, R. Juza, Z. Anorg. Allgem. Chem. 391 (3) (1972) 271–279.
[18] K. Miwa, N. Ohba, S. Towata, Phys. Rev. B71 (2005) 195109-1.
[19] J.B. Yang, X.D. Zhou, Q. Cai, W.J. James, W.B. Yelon, Appl. Phys. Lett. 88 (2006) 041914-1.
[20] A.C. Larson, R.B. Von Dreele, General Structure Analysis System (GSAS), Los Alamos National Laboratory Report LAUR 86-748 (2000).
[21] B.H. Toby, J. Appl. Cryst. 34 (2001) 210–213.